Hindawi
Shock and Vibration
Volume 2020, Article ID 4386259, 16 pages
https://doi.org/10.1155/2020/4386259

Research Article

Research on the Influence of External Parameters of Fan-Type Nozzle on Water Jet Performance

Baofu Kou,[1] **Pengliang Huo**,[1] **and Xiaohua Hou**[2]

[1]*School of Mechanical Engineering, Taiyuan University of Science and Technology, Taiyuan 030024, China*
[2]*Vocational Education Center of Yangquan Coal Group, Yangquan, Shanxi 045000, China*

Correspondence should be addressed to Baofu Kou; koubaofu2004@163.com

Received 9 January 2020; Revised 4 July 2020; Accepted 2 September 2020; Published 22 September 2020

Academic Editor: Fabio Rizzo

At present, high-pressure water jet technology occupies a very important position in the automobile washing industry. Some automatic washers cannot meet the washing requirements in the washing process due to unreasonable arrangement of nozzles on their spray rods. Based on the theory of computational fluid dynamics (CFD), the internal and external flow field model of the nozzle are established in this paper. Fluent is used to simulate and analyze the flow field, and the external parameters of the nozzle on the side spray bar of the automatic automobile washer are optimized. The simulation results show that after the nozzle and the normal line of the automobile surface are inclined at a certain angle, the target surface is affected not only by normal striking force but also by tangential pushing force, which makes stains easier to remove. The washing effect is the best when the nozzle is inclined 30° to the normal line of the automobile surface. Increasing the nozzle inlet pressure will increase the dynamic pressure on the automobile surface, but the increase of dynamic pressure will decrease after increasing to a certain pressure. The inlet pressure has little effect on the area covered by water jet. The reasonable matching results of jet angle, nozzle spacing, and nozzle distance from the automobile surface (target distance) obtained by numerical simulation can not only make the automobile surface completely covered and cleaned but also ensure less jet interference and no waste of water from adjacent nozzles. The above research conclusions can provide a basic theoretical basis for the optimal design of automatic automobile washing.

1. Introduction

With the development of society, the number of automobiles is increasing rapidly, and the related research on vehicle maintenance is increasing day by day [1, 2]. Among them, the daily washing quantity and frequency are more numerous [3]. In the past, manual washing could not meet this large number and high frequency of automobile washing. At present, automatic automobile washing is divided into contact type and noncontact type. Although contact type can quickly remove stains on the automobile, hard particles (such as sand, small stones, and fine steel wires) often contained in stains on the automobile will get involved in the washing head, which results in the damage to the automobile. The noncontact type uses high-pressure water sprayed by high-pressure fan-type nozzles for washing, which will not cause friction damage to the automobile. High-pressure water jet washing is the key technology of automobile washer [4, 5]. It has been widely used because of its strong decontamination capability, wide application range, no environmental pollution, and easy automation [6–10]. It provides the basis for the automatic control of the car washing industry [11–14]. The high-pressure jet washer uses the high-pressure pump to provide pressure, and the high-pressure water flow is ejected from the nozzle [8, 15, 16].

At present, relevant scholars at home and abroad have done a lot of research on the jet characteristics of the nozzle according to its internal structural parameters. Wen et al. [17–19] analyzed the influence of the structural parameters of the nozzle on the hydraulic performance and concluded that the impact force of the water jet generated by the straight cone nozzle increases with the increase of the nozzle outlet diameter. The cylindrical outlet section of the straight

cone nozzle is conducive to improving its hydraulic performance, which makes its hydraulic performance better than that of the cone nozzle. Nadeem et al. [20, 21] used particle image velocimetry and computational fluid dynamics methods to obtain the fact that the particles in the central area of the spray plate have the largest kinetic energy, and the area has the ability to hit the correct target on the surface of the plant, while the liquid particles around the central area have the velocity of smaller kinetic energy and minimum kinetic energy and have the greatest chance to deviate from the target during spraying. Fuchs et al. [22] studied two different pulsating washing methods from the perspective of washing efficiency, thus reducing washing cost and saving operation time. Chee et al. [23] quantitatively analyzed the influence of jet length and wall curvature on the flow pattern of impinging water jet and preliminarily studied the jet washing effect. The length of time required to establish a stable flow is described. Nie et al. [24] obtained through numerical simulation that the jet impact pressure is larger when the nozzle outlet diameter is 2–7 times. Kermanpur et al. [25, 26] showed that, combined with industrial data and using the artificial neural network model, the sensitivity analysis of the influence of different injection angles, pressures, vertical heights, and water flow rates of phosphorus removal nozzles on jet striking force was carried out. In the range of 7 times the outlet diameter, the impact pressure is significantly reduced. Dou et al. [27] proposed a new type of self-propelled nozzle suitable for pipeline washing, analyzed the influence of the number, included angle, and eccentricity of nozzles on the pipeline washing effect, and proposed a reasonable arrangement to improve the efficiency of high-pressure water washing. In order to achieve the best washing effect, Liu et al. [28] carried out experimental research and analysis on the working state of the nozzle under different flow rates, from four aspects: cavitation form, pressure pulse frequency, velocity fluctuation amplitude, and erosion effect. In order to understand the influence of structural parameters of high-pressure water jet nozzle on jet performance, the influence of various structural parameters of nozzle on jet performance was simulated and verified by experiments with outlet expansion angle, cone hole depth, and inlet contraction angle as reference factors and injection angle and jet flow rate as evaluation indexes by Liang and Gao [29]. For the sake of research on the effects of the inclination angle of forward nozzles and standoff distance, Liu et al. [30] adopted the ANSYS Fluent combined with RNG turbulence model to analyze the multinozzle jets flow field. The results indicate that the components of axial velocity and tangential velocity of forward nozzle jets are different from inclination angles of forward nozzles.

At present, there are many researches on the influence of the internal structural parameters of the washing nozzle on its washing effect at home and abroad, but there are few researches on the influence of the external parameters of the fan-type nozzle for washing on its jet performance. However, in the actual application process, the washing effect of the high-pressure water jet on the automobile also depends on the distance between the nozzle and the automobile, the water flow pressure, the nozzle arrangement distance, the included angle between the nozzle and the normal line of the target surface, and so on.Through the dynamic simulation analysis of different nozzle inlet pressures, different target distances, different included angles, and different nozzle arrangement spacing, the influence law of each parameter on the automobile washing effect is summarized and its rationality is verified by experimental ways, which provides certain theoretical guidance for the practical application of high-pressure water jet automobile washing, so as to achieve ideal automobile washing effect.

2. Characteristics and Mathematical Model of Nozzle Water Jet

2.1. Water Jet Distribution Structure of Automobile Washing Nozzle. Figure 1 is a physical diagram of the spray rod and nozzle of an automatic automobile washer. The nozzle water jet structure [31] is shown in Figure 2. After the water jet is ejected from the slit of the nozzle, due to the huge speed difference between the water jet and the surrounding air and the exchange of energy and mass with the air, the ejected water jet continuously diffuses to the surrounding. Then the boundary of the jet widens, the velocity decreases, and the area where the velocity keeps the initial velocity unchanged also decreases continuously. The boundary with zero velocity is the outer boundary of the jet.

The water jet is roughly divided into three jet sections, which are successively divided into the initial section, the basic section, and the dissipation section from the nozzle outlet. The initial section of water jet is the jet section from the outlet of the nozzle to the complete disappearance of the velocity core. The axial dynamic pressure, velocity, and density remain basically unchanged in the jet core area. Therefore, the initial section of water jet is generally used for material cutting. The mixing zone of the water jet is the zone where the velocity core zone is removed from the initial section of the jet. The pressure and velocity of water jet flow in the basic section of water jet gradually decrease, but the cavitation situation in the basic section of water jet is not too serious, and basically, the jet can be kept relatively compact. Surface processing, washing, and derusting are commonly used in engineering. The cavitation of the jet is quite serious in the last part of the dissipation section of the water jet. The two are completely mixed and cannot keep the jet relatively compact. This area is mainly used for cooling and dust removal.

2.2. Mathematical Model. For high-pressure water jet washing, assuming that water is an incompressible steady-state flow, the continuity equation is

$$\frac{\partial u}{\partial x} + \frac{\partial v}{\partial y} + \frac{\partial w}{\partial z} = 0, \tag{1}$$

where u, v, and w are the three velocity components of x, y, and z, respectively, m/s.

Figure 1: The physical diagram of the side spray bar of an automatic automobile washer.

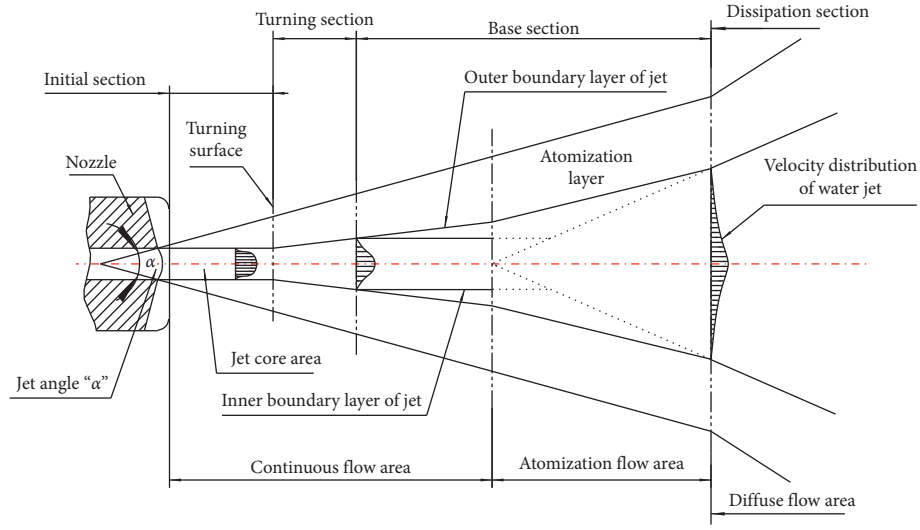

Figure 2: The jet distribution structure diagram of the nozzle.

The momentum equation is

$$\begin{cases} f_x - \dfrac{1}{\rho}\dfrac{\partial p}{\partial x} + \dfrac{\mu}{\rho}\left(\dfrac{\partial^2 u}{\partial x^2} + \dfrac{\partial^2 u}{\partial y^2} + \dfrac{\partial^2 u}{\partial z^2}\right) = \dfrac{\partial u}{\partial t} + u\dfrac{\partial u}{\partial x} + v\dfrac{\partial u}{\partial y} + w\dfrac{\partial u}{\partial z}, \\ f_y - \dfrac{1}{\rho}\dfrac{\partial p}{\partial y} + \dfrac{\mu}{\rho}\left(\dfrac{\partial^2 v}{\partial x^2} + \dfrac{\partial^2 v}{\partial y^2} + \dfrac{\partial^2 v}{\partial z^2}\right) = \dfrac{\partial v}{\partial t} + u\dfrac{\partial v}{\partial x} + v\dfrac{\partial v}{\partial y} + w\dfrac{\partial v}{\partial z}, \\ f_z - \dfrac{1}{\rho}\dfrac{\partial p}{\partial z} + \dfrac{\mu}{\rho}\left(\dfrac{\partial^2 w}{\partial x^2} + \dfrac{\partial^2 w}{\partial y^2} + \dfrac{\partial^2 w}{\partial z^2}\right) = \dfrac{\partial w}{\partial t} + u\dfrac{\partial w}{\partial x} + v\dfrac{\partial w}{\partial y} + w\dfrac{\partial w}{\partial z}, \end{cases} \tag{2}$$

where f_x, f_y, and f_z are the components of unit mass force on 3 coordinate axes, respectively; ρ is the density of water, kg/m^3; μ is the dynamic viscosity of water, kg/m·s.

Water jet automobile washing belongs to the gas-liquid two-phase flow movement. First of all, it is necessary to judge whether it is a laminar flow or turbulent flow. In multiphase flow, each relevant parameter can be expressed by the following equation:

$$R_e = \frac{\rho v \quad D}{\mu}, \tag{3}$$

where R_e is the Reynolds number; v is the velocity of water at the nozzle inlet, m/s, generally about 100 m/s; D is the diameter of nozzle inlet, about 3 mm; $\mu = 0.001$ kg/m·s.

Substituting various data, R_e is 229400, which is much greater than 2300, so this jet belongs to highly turbulent flow. The standard k–ε is selected as the turbulence calculation model. The relevant calculation equation is as follows:

$$\begin{cases} \rho \dfrac{dk}{dt} = \dfrac{\partial}{\partial y_j}\left[\left(\mu + \dfrac{\mu_t}{\delta_k}\right)\dfrac{\partial k}{\partial x_i}\right] + G_k + G_b - \rho\varepsilon - Y_M + S_k, \\ \rho \dfrac{d\varepsilon}{dt} = \dfrac{\partial}{\partial x_i}\left[\left(\mu + \dfrac{\mu_t}{\delta_\varepsilon}\right)\dfrac{\partial \varepsilon}{\partial x_i}\right] + C_{1\varepsilon}\dfrac{\varepsilon}{k}\left(G_k + C_{3\varepsilon}G_b\right) - C_{2\varepsilon}\rho\dfrac{\varepsilon^2}{k} + S_\varepsilon, \end{cases} \tag{4}$$

where G_k is the turbulent kinetic energy generated by the laminar velocity gradient; G_b is the turbulent energy generated by the buoyancy; Y_M is the wave generated by the transition diffusion in the compressible turbulence; S_k and S_ε are user-defined source terms; $C_{1\varepsilon}$, $C_{2\varepsilon}$, and $C_{3\varepsilon}$ are the viscous diffusion coefficients (empirical constants), which are, respectively, 1.44, 1.92, and 0.09; δ_k is the Prandtl number corresponding to the turbulent kinetic energy k, $\delta_k = 10$; δ_ε is the Prandtl number corresponding to dissipation rate, $\delta_\varepsilon = 1.3$; μ_t is turbulent viscosity, $\mu_t = \rho C_\mu k^2/\varepsilon$ [32].

3. Establishment and Verification of Simulation Model

3.1. 3D Model. The high-pressure water jet discussed in this paper belongs to obvious gas-liquid two-phase flow with obvious interface stratification, and the jet also belongs to free-surface flow. Based on the above mathematical model, VOF model and standard turbulent k–ε model are selected for analysis in simulation.

In order to study the water-gas two-phase flow field when the water jet leaves the nozzle and enters the air, SOLIDWORKS software is used to carry out 3D model of the internal and external flow fields. In order to better connect the internal flow fields with the external flow fields, a triangular prism is established outside the fan-type nozzle as the transition area of the internal and external flow fields [15], and the 3D model is shown in Figure 3.

3.2. Mesh Generation and Fluent Boundary Condition Setting. In the process of mesh division, tetrahedral mesh and hexahedral mesh are combined, the mesh is encrypted at nozzles and triangular prisms, and an expansion layer is set up at the outflow field. Finally, the skewness of the mesh is observed to be about 0.2, and the mesh quality measurement grade is shown in Table 1 [32], which shows that it belongs to the category of "very good." The orthogonal mass is about 0.9, and the numerical range of orthogonal mass is 0~1; the closer to 1, the better. The above shows that the lattice quality meets the requirements [32]. The divided mesh is shown in Figure 4.

The boundary condition setting is shown in Figure 3. Since air fills the whole outflow field in the initial state, air is selected as the main phase and water fluid as the second phase in order to solve the near-real situation. Select the inlet boundary pressure of the nozzle to be 6–12 MPa, and set the volume fraction of inlet water to be 1, i.e., the nozzle is filled with water in the initial state, the outlet pressure is set to 1 atmosphere (i.e., the relative static pressure is zero), and the external flow field is filled with air at the beginning of

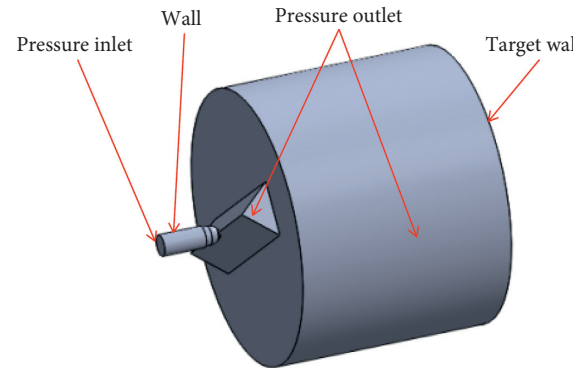

Figure 3: 3D model of nozzle and external flow field.

injection. The wall surface adopts the standard nonslip wall surface, the standard wall surface function simulates the near-wall effect, and the SIMPLE pressure-velocity coupling semi-implicit algorithm is used to solve the problem. The jet medium is water, the density at room temperature is 998 kg/m^3, and the dynamic viscosity is 0.001 kg/(m·s). The air density is 1.225 kg/m^3, and the dynamic viscosity is 1.789 kg/(m·s) [33]. After setting the boundary conditions, the first-order upwind discrete scheme is used to solve the problem. In order to make the calculation more accurate, the monitoring accuracy is adjusted to 0.0001, and the number of iteration steps is set to 1000 steps. After 1000 steps, the residual tends to be stable and the operation is finished.

3.3. Verify the Correctness of the Model. For continuous jet, the Bernoulli equation is adopted between the inner and outer two points of nozzle outlet cross section, ignoring the height difference between the two points, and the following relation [34] can be obtained:

$$\frac{p_1}{\rho_1} + \frac{v_1^2}{2} = \frac{p_2}{\rho_2} + \frac{v_2^2}{2}, \tag{5}$$

where p_1 and p_2 are the static pressure inside and outside the nozzle; v_1 and v_2 are the average flow velocity inside and outside the nozzle.

Applying the continuous equation to two points, the following relation can be obtained:

$$\rho_1 v_1 A_1 = \rho_2 v_2 A_2. \tag{6}$$

For the convenience of theoretical analysis, the nozzle flow path can be a circular tube structure; that is, $A = \pi d^2/4$; assuming $\rho_1 = \rho_2$, the following relationship can be deduced by combining (5) and (6):

$$v_2 = \sqrt{\frac{2(p_1 - p_2)}{\rho\left[1 - (d_2/d_1)^4\right]}}. \tag{7}$$

For the water jet used for washing, because $p_1 >> p_2$, $(d_2/d_1)^4 << 1$, and $\rho = 998\,\text{kg/m}^3$, the relevant values are substituted into (7), and the simplified expression of jet velocity is obtained:

Table 1: Skewness mesh quality grades [21].

0–0.25	0.25–0.50	0.50–0.80	0.80–0.95	0.95–0.98	0.98–1.00*
Excellent	Very good	Good	Acceptable	Bad	Inacceptable*

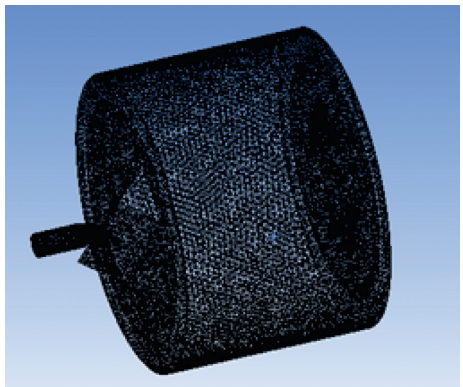

Figure 4: Mesh model of nozzle and external flow field.

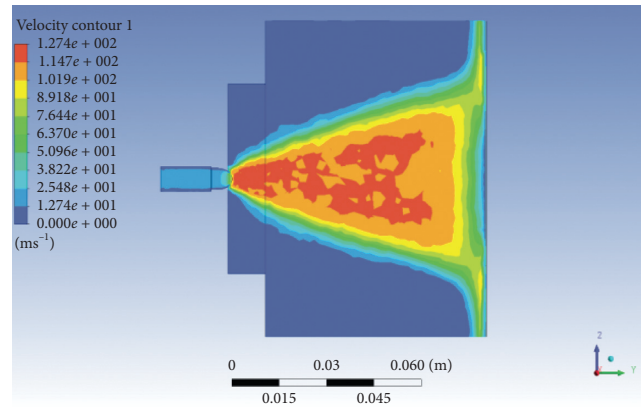

Figure 5: Water jet velocity nephogram with inlet pressure of 8 MPa.

$$v_t = 44.77\sqrt{p}, \tag{8}$$

where p is the static pressure at the nozzle inlet; v_t is the nozzle outlet velocity.

From equation (8), when the static pressure at the inlet is 8 MPa, the velocity at the outlet of the nozzle is 126.60 m/s.

In order to verify the correctness of the simulation model, it is necessary to compare the value calculated by the above formula with the simulation result. Therefore, both solutions are set as the static inlet pressure 8 MPa. The simulation results are as shown in Figure 5. The velocity at the nozzle outlet is 127.40 m/s according to the velocity nephogram. The error $\Delta = (127.4–126.6)/126.6 = 0.632\%$. The simulation results are very close to the theoretical calculation results, which show that the model is reliable.

4. Numerical Simulation Results and Discussion

4.1. Simulation Analysis and Comparison of Different Target Distances. As can be seen from Figure 1, the water jet velocity and dynamic pressure in the basic section gradually decrease with the axial target distance (the distance from the nozzle outlet to the automobile surface). Obviously, the choice of target distance has a great influence on the washing effect. The dynamic pressure on the target surface is an important characteristic of water jet, which represents the striking force of water jet on the target surface.

The inlet pressure is selected to be 8 MPa, and the external flow field is simulated and analyzed under the conditions that the target distances are 60 mm, 70 mm, 80 mm, and 100 mm, respectively. The dynamic pressure cloud images of the target surface under different target distances are obtained as shown in Figure 6, and the radial dynamic pressure curves of the target surface under different target distances are shown in Figure 7.

In order to achieve the best washing effect, the dynamic pressure on the target surface should be as large as possible. As can be seen from Figure 6, these dynamic pressures vary significantly under the same inlet pressure and different target distances. When the target distances are 60 mm, 70 mm, 80 mm, and 100 mm, the corresponding maximum dynamic pressure values at the target center are 125400 Pa, 111300 Pa, 96170 Pa, and 72330 Pa, respectively. Although the washing capability of the water jet decreases with larger target distance, the coverage area of the water jet increases, and the area of the automobile that can be cleaned increases. By observing Figures 6 and 7, it can be seen that when the target distance is 60 mm, the water jet reaching the target surface has a reverse impact force that partially cancels the forward water jet reaching the target surface due to the nozzle being too close to the surface of the automobile, making the dynamic pressure on the target surface uneven. With the increase of target distance, the dynamic pressure on the target surface begins to decrease, but the nonuniformity of the dynamic pressure value is obviously alleviated. On the premise of ensuring that the dynamic pressure on the target surface is large enough and considering the uniformity of the dynamic pressure on the target surface, relatively speaking, 70 mm should be selected as the optimal target distance under this working condition.

4.2. Comparison of Simulation Analysis of Different Inlet Pressures. The target distance is 70 mm, and the external flow field is simulated under the conditions of inlet pressures

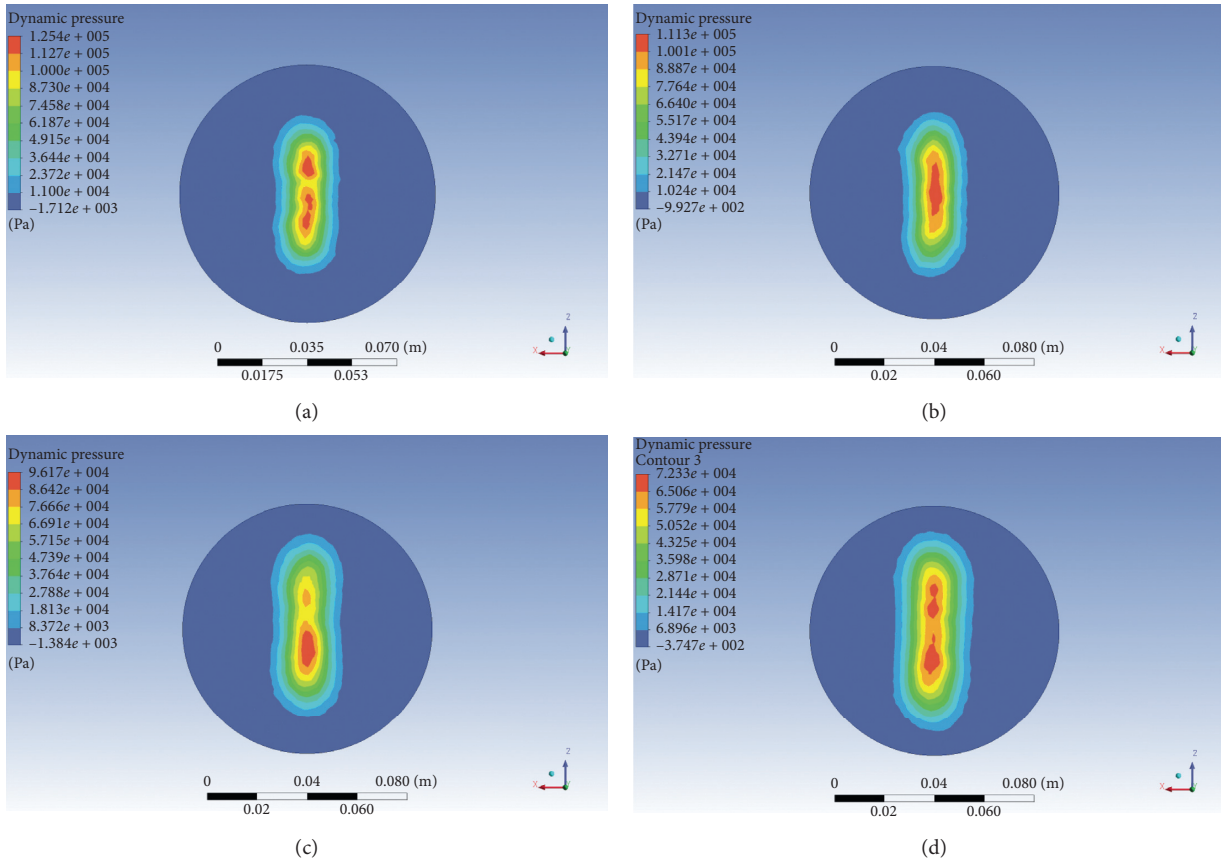

Figure 6: Dynamic pressure nephogram of target surface at different target distances. (a) 60 mm. (b) 70 mm. (c) 80 mm. (d) 100 mm.

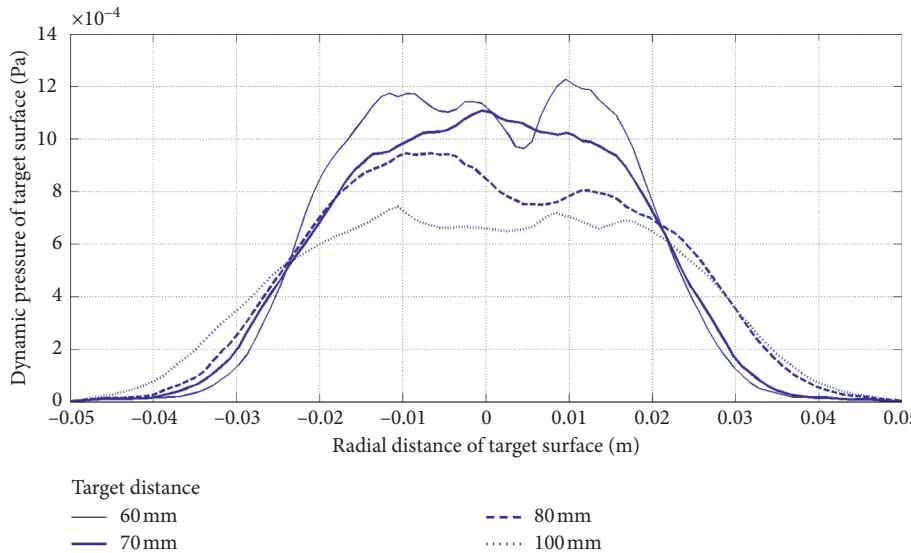

Figure 7: Radial dynamic pressure curve of target surface at different target range.

of 6 MPa, 8 MPa, 10 MPa, and 12 MPa, respectively. The dynamic pressure nephogram of the target surface under different inlet pressures is obtained as shown in Figure 8, and the axial velocity distribution under different inlet pressures is shown in Figure 9.

As can be seen from Figure 8, when the inlet pressure changes from 6 MPa to 8 MPa, the target surface dynamic pressure increase rate is 33.18%, when the inlet pressure changes from 8 MPa to 10 MPa, the target surface dynamic pressure increase rate is 24.89%, and when the inlet pressure

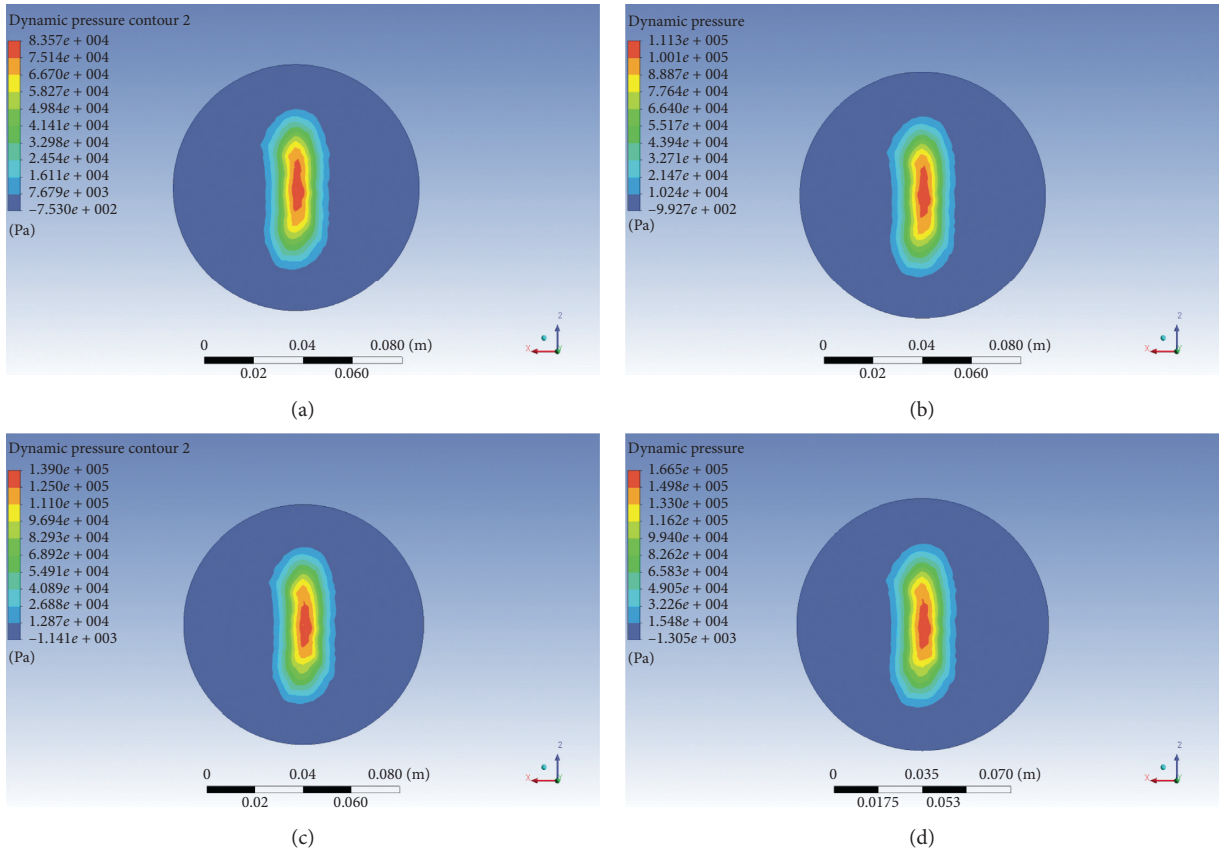

Figure 8: Target dynamic pressure nephogram under different inlet pressure. (a) 6 MPa. (b) 8 MPa. (c) 10 MPa. (d) 12 MPa.

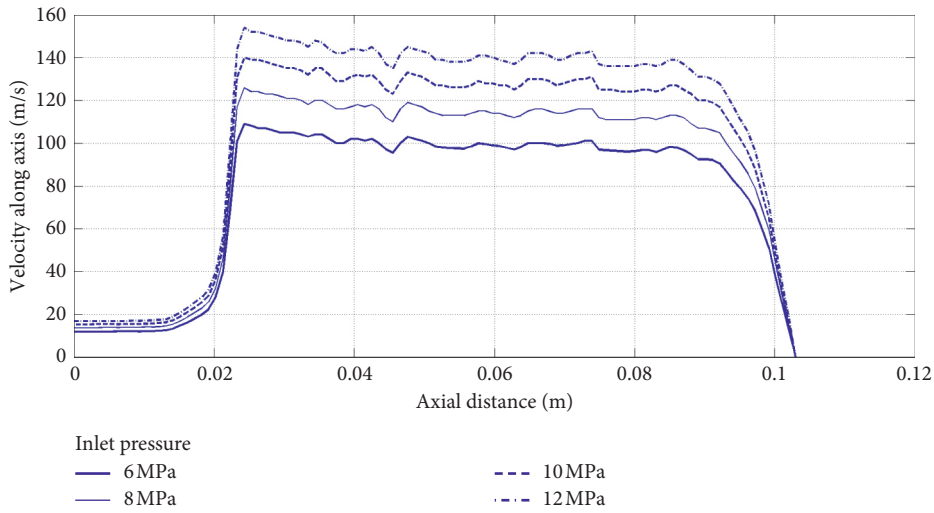

Figure 9: Axial velocity curves under different inlet pressures.

changes from 10 MPa to 12 MPa, the target surface dynamic pressure increase rate is 19.78%. It can be concluded that the increase rate of the dynamic pressure on the target surface decreases with the increase of the inlet pressure; under the condition of a certain target distance, the area covered by water jets with different inlet pressures is basically the same. As seen in Figure 9, when the inlet pressure starts to increase from 6 MPa, the axial speed also increases. The speed increase from 6 MPa to 8 MPa is larger than that of from 8 MPa to 10 MPa or 10 MPa to 12 MPa. Comparing with the speed before reaching the target surface, it can be seen that the decay speed of the axial speed before reaching the target surface becomes faster with the increase of the inlet pressure. Therefore, considering the dynamic pressure of the target

surface and the axial speed, the inlet pressure is 10 MPa as the optimal pressure under this working condition. In conclusion, when the target distance is fixed, the coverage area of water jet has nothing to do with the inlet pressure; with the increase of inlet pressure, the dynamic pressure and axial velocity of the target increase continuously, but their increasing rate decreases.

4.3. Simulation Analysis and Comparison of Different Included Angles. At present, the spray rod nozzle of the car wash is perpendicular to the surface of the automobile, so that the surface of the automobile is mainly subject to normal strike force and little tangential strike force during the washing process, and some stubborn stains are not easy to be cleaned off. In the process of water jet washing, it should be considered that inclining the jet direction of the nozzle to the target surface (automobile surface) at a certain angle will greatly enhance its washing effect. At this time, the cleaned surface is affected by the impact forces and shear forces of the water jet. When the water jet hits the target surface, the velocity is decomposed into two directions perpendicular to the target surface and parallel to the target surface. The velocity perpendicular to the target surface will strike and loosen the attachments on the target surface, and the velocity parallel to the target surface will wash away the attachments.

In order to realize the simulation of outflow field under different included angles, the normal included angles between nozzle and target surface are 0°, 15°, 30°, and 45° through different angles of target surface inclination. The schematic diagram of the model is shown in Figure 10, and the 3D model is shown in Figure 11.

As can be seen from Figure 12, regardless of the inlet pressure, the following conclusions can be drawn. The dynamic pressure of the target surface decreases with the increase of the inclination angle. From 15° to 30°, the decreased amplitude is small, but from 30° to 45°, the decrease amplitude increases. This is due to the fact that part of the kinetic energy is absorbed by the target surface after the water jet impacts the target surface at a certain angle, and the other part of the kinetic energy produces a tangential force on the stain, resulting in a decrease in the dynamic pressure on the normal target surface. By observing Figure 13, it can be seen that when the inclination angle is 0°, the speed of the water jet reaching the target surface in the tangential advancing direction is very small. After inclining by a certain angle, the speed of the water jet reaching the target surface in the tangential advancing direction of the nozzle gradually increases and reaches the maximum when the inclination angle is 30°. Therefore, considering the velocity distribution and the dynamic pressure of the target surface comprehensively, 30° is taken as the optimal included angle.

4.4. Comparison of Simulation Analysis with Different Spacing. When arranging nozzles, the influence of nozzle spacing on the external flow field should be considered. If the nozzle spacing is too small, the edge water jet of the fan-type external flow field will interfere, thus affecting the washing effect. If the nozzle spacing is too large, the fan-type outflow

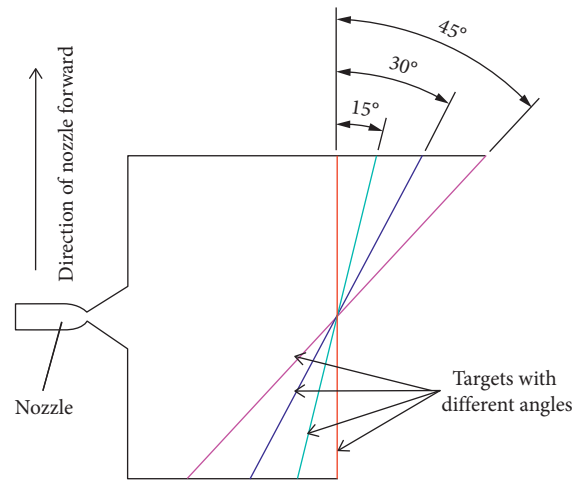

Figure 10: Model schematic diagram different from normal angle of target surface.

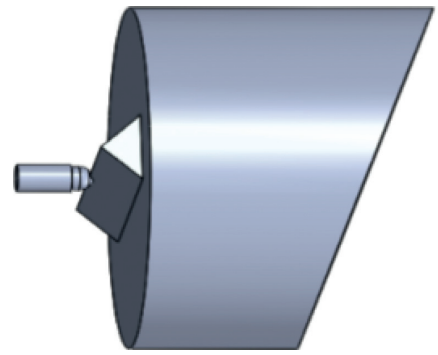

Figure 11: 3D model with inclined angle.

field cannot cover all washing surfaces and cannot meet the washing requirements. In this paper, the nozzle spacing is simulated by establishing a 3D model as shown in Figure 13.

By observing Figures 14–16, when the nozzle spacing is 100 mm, the watersheds of the two nozzles hardly intersect, so that some areas of the automobile surface between the two nozzles cannot be effectively cleaned. With the decrease of the nozzle spacing, the outflow fields of the two nozzles begin to intersect, so that the target surface between the two nozzles can be effectively cleaned. By looking at Figure 17, it is shown that, with the decrease of nozzle spacing, the interference degree of adjacent water jets increases gradually. Therefore, considering the velocity distribution and the dynamic pressure on the target surface, it is more appropriate to select the nozzle spacing of 70 mm under this working condition. The above results show that the target distance and nozzle distance must be matched to ensure the washing effect. It is necessary to discuss the relationship between the target distance and nozzle distance.

4.5. Relationship between Target Distance and Shooting Width under Different Jet Angles. As can be seen from Figure 8, the inlet pressure of the nozzle has little influence on the shooting width (range covering the target surface) of the

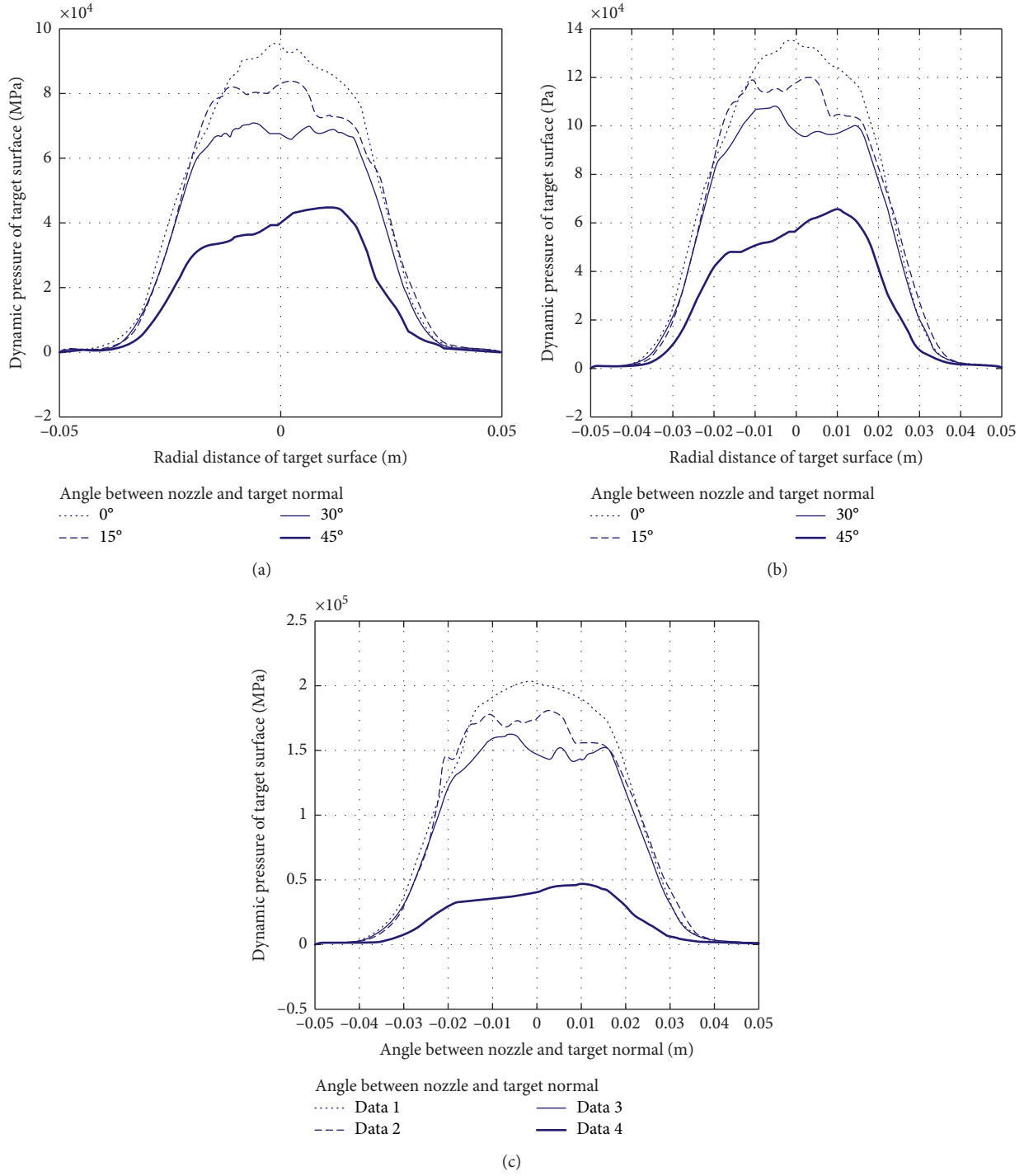

Figure 12: Radial dynamic pressure curves of target surface at different angles. (a) Interpressure 7 MPa. (b) Interpressure 10 MPa. (c) Interpressure 15 MPa.

water jet. As can be seen from Figures 15 and 16, the target distance has a great influence on the shooting width (range covering the target surface) of the water jet. In addition, practical application and theoretical analysis show that the jet angle α of the nozzle will inevitably affect the jet width of the water jet (covering the range of the target surface). Based on the above model, this paper discusses the relationship between target distance and shooting width under different jet angles by numerical simulation. When the jet angle α is 15°, 30°, 45°, and 60° and the target distance is adjusted to 50 mm, 100 mm, 150 mm, 200 mm, 250 mm, 300 mm, 350 mm, 400 mm, 450 mm, and 500 mm, respectively, the shooting width is investigated to find out the matching relationship between the target distance and the shooting width. The solution result is shown in Figure 18.

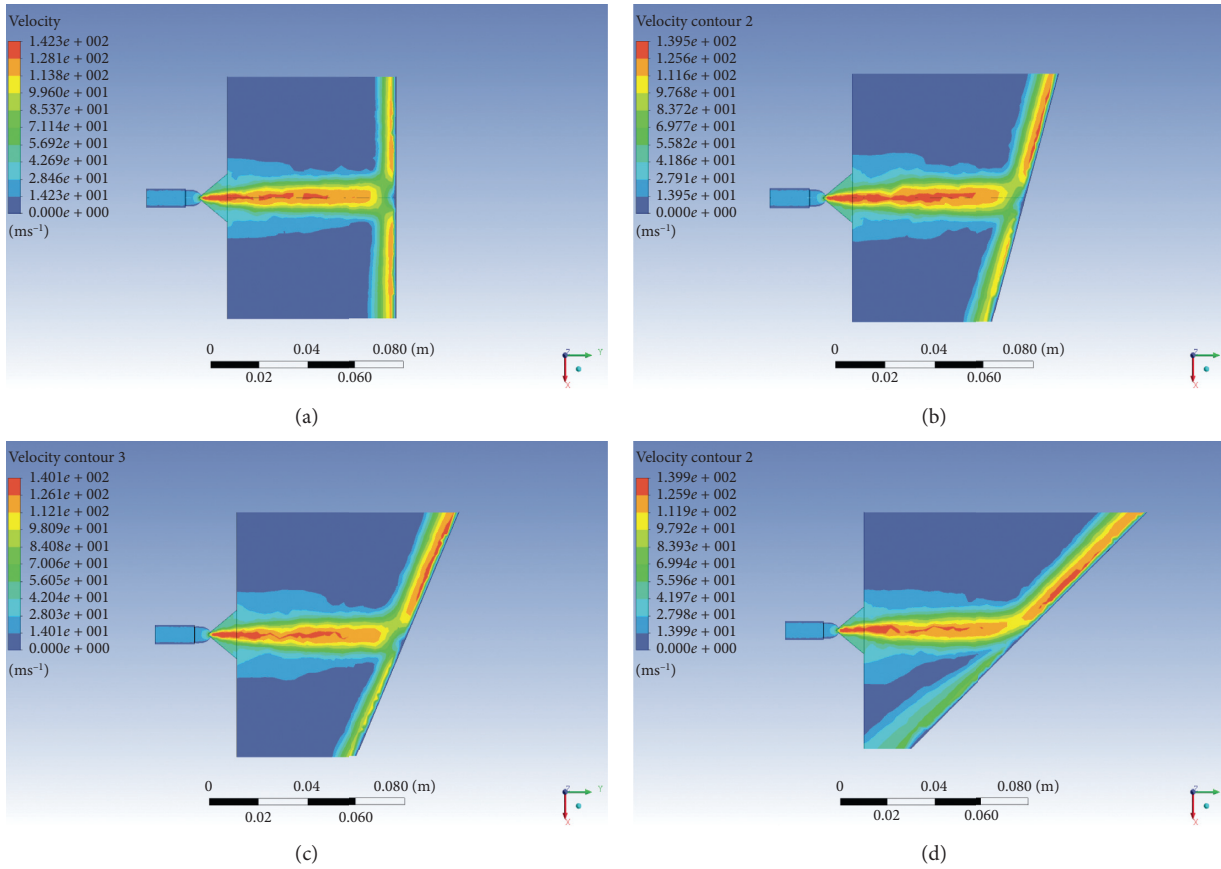

Figure 13: Velocity nephogram at different angles. (a) 0°. (b) 15°. (c) 30°. (d) 45°.

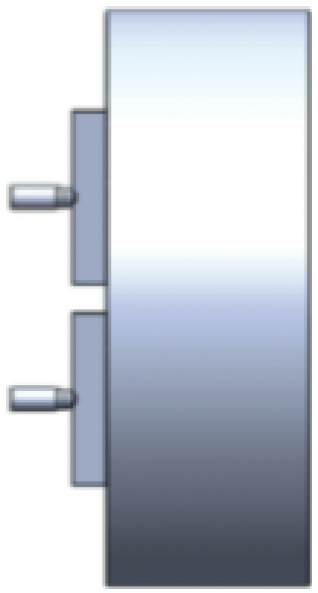

Figure 14: 3D model with different spacing.

From the solution rule curve in Figure 18, it can be seen that no matter what the jet angle is, the width of the water jet will increase with the increase of the target distance. When the jet angle is small, the increase rate of jet width is small, and the increase rate also increases with the increase of jet angle, but the increase rate tends to be stable when the jet angle is greater than or equal to 45°. Only when the nozzle spacing is less than or equal to the jet width, the whole automobile surface can be completely covered by the water jet to ensure that the automobile is completely cleaned. However, Figure 18 can be used as the theoretical basis for matching the jet angle, nozzle spacing, and the distance between the nozzle and the automobile surface (target distance). In actual automobile washing, the nozzle spacing on the spray rod is generally premade (it will not change during automobile washing). If the nozzle spacing is too small, the jet coverage area can be effectively increased, but the number of nozzles on the spray rod of the same length will inevitably increase and the water consumption will also rise sharply. As can be seen from Figure 15, when the nozzle spacing is too large, part of the automobile surface cannot be covered by water jet. Therefore, when washing the car, the distance (target distance) between the nozzle on the spray rod and the surface of the automobile can be adjusted to ensure that the jet width value is always greater than the nozzle spacing, thus achieving the purpose of washing without dead corners. For the automatic automobile washer, the regular curve in Figure 18 can be input into the electronic control integrated control module, and dynamically adjusting the distance (target distance) between the spray

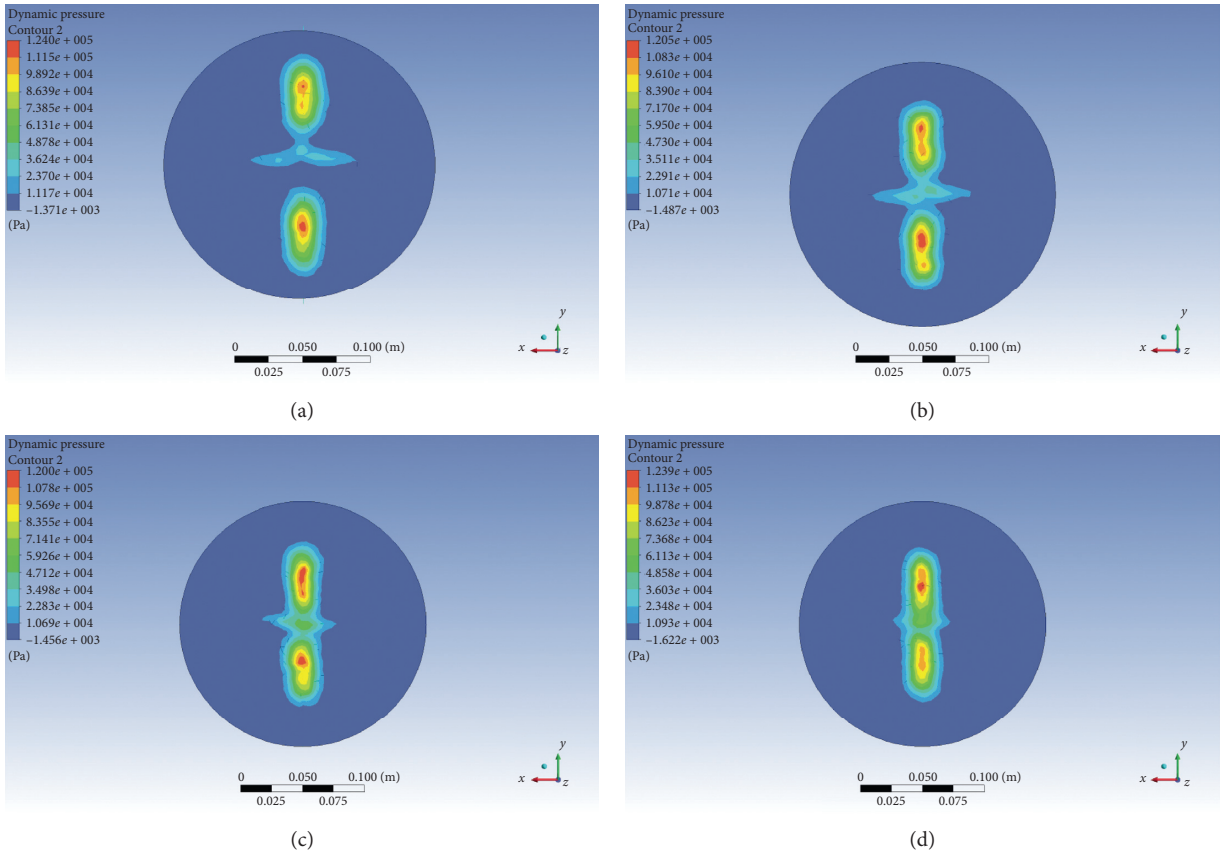

Figure 15: Dynamic pressure nephograms of target surfaces with different spacing. (a) 100 mm. (b) 80 mm. (c) 70 mm. (d) 60 mm.

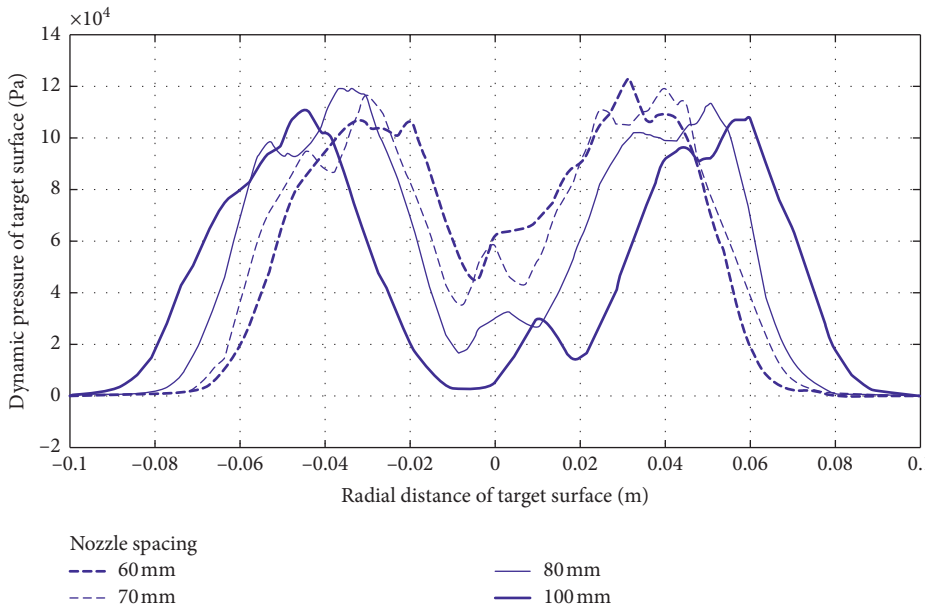

Figure 16: Radial dynamic pressure of target surface at different spacing.

rod and the automobile not only makes the automobile surface fully covered and cleaned but also ensures less jet interference from adjacent nozzles and no waste of water.

4.6. Test Verification. Since the impact force of water jet on the automobile cannot be accurately detected, the cleanliness of the automobile is used to check whether the impact force

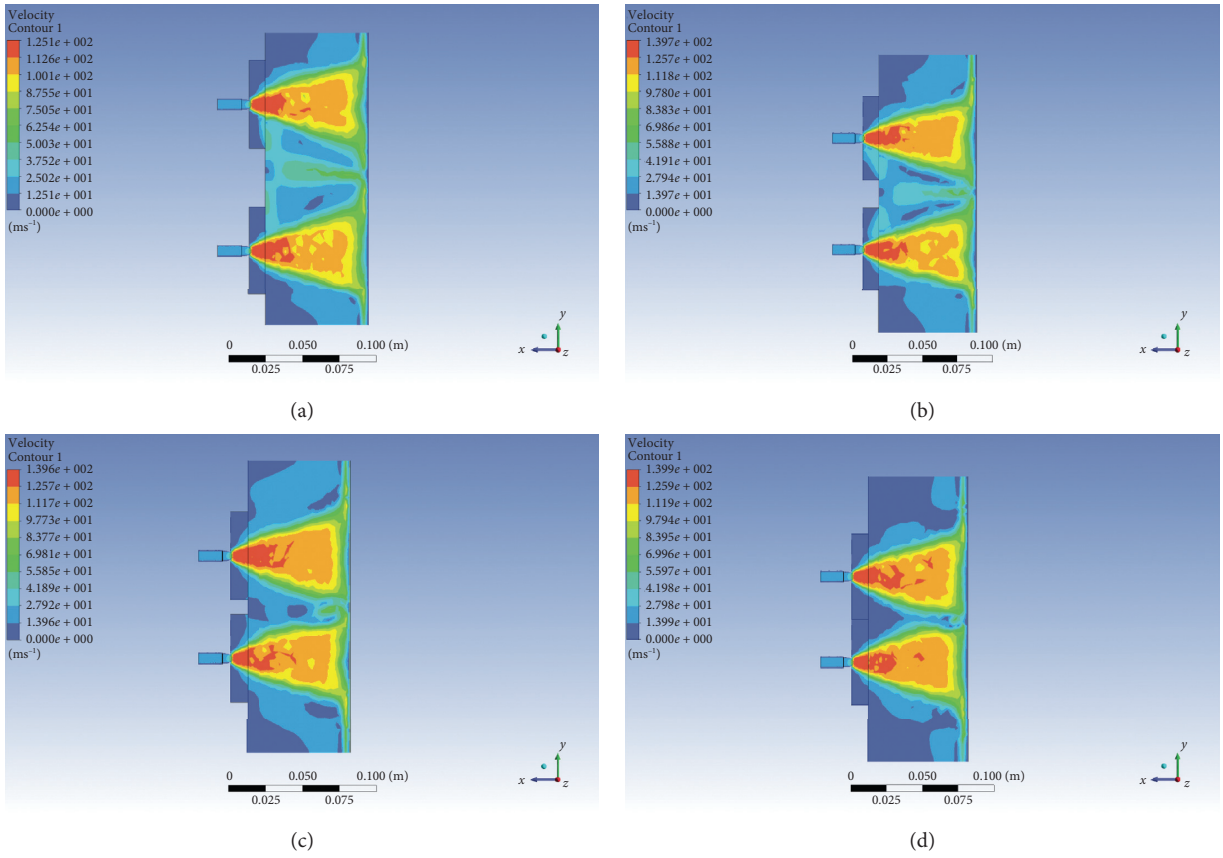

Figure 17: Velocity nephogram with different spacing. (a) 100 mm. (b) 80 mm. (c) 70 mm. (d) 60 mm.

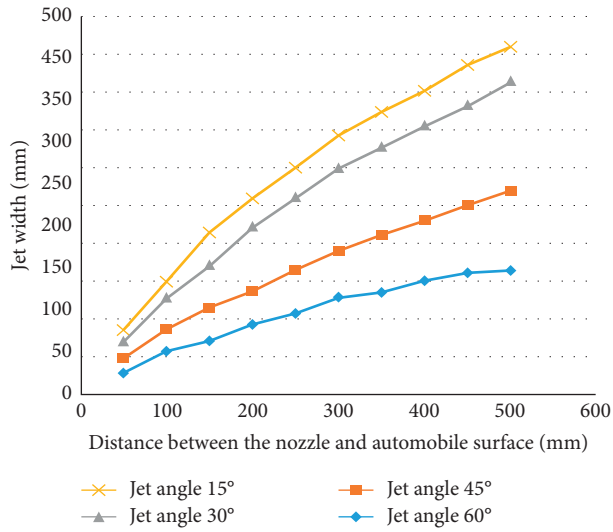

Figure 18: Relationship curve between jet target distance and jet width under different jet angles.

is appropriate. Taking an automatic automobile washing workshop as the test object, the original automatic automobile washer has 15 nozzles with an incidence angle of 45°, a distance between the nozzle and the automobile on the automobile washing spray rod of about 300 mm, a normal angle between the nozzle jet direction and the target surface (automobile surface) of 0°, and a distance between adjacent nozzles of 150 mm. The inlet pressure can be adjusted according to the degree of stains on the automobile. The layout of the on-site automatic automobile washer is shown in Figure 19. According to the above theoretical research conclusions, the external parameters of the spray rod and nozzle are adjusted. Firstly, according to the conclusion of Figure 18, the spacing between the on-site nozzles and the

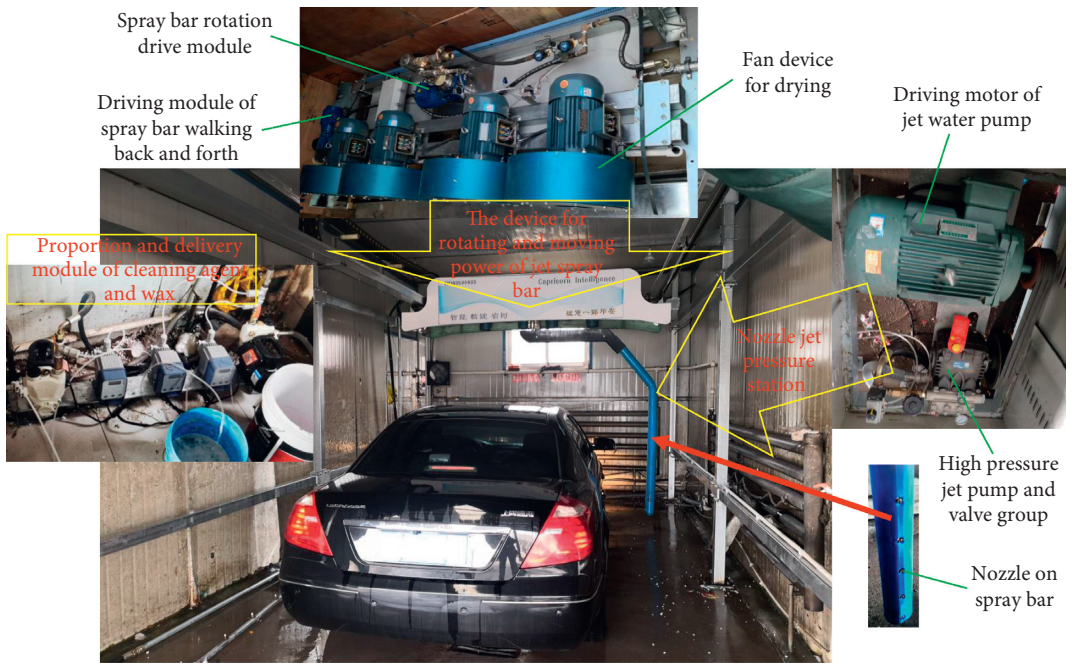

Figure 19: Layout of on-site automatic automobile washer.

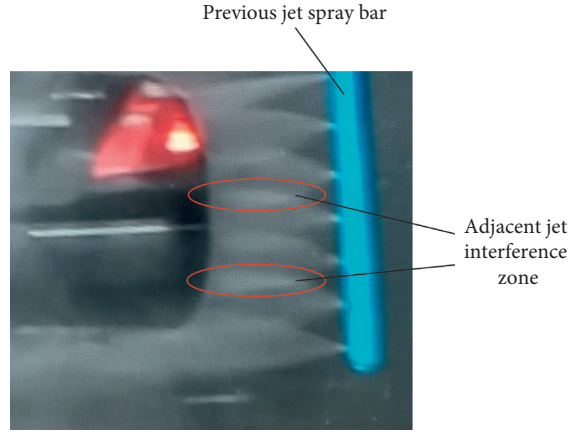

Figure 20: Nozzle jet before modification.

automobile is 300 mm, and the spacing between the adjacent nozzles on the spray rod is 300 mm, totaling 8 nozzles. According to the conclusion of Figures 12 and 13, the angle between the nozzle jet direction and the target surface (automobile surface) is 30°.

Under the same condition of washing the automobile, the following conclusions can be drawn through the comparison before and after the renovation: (1) The water consumption after the renovation is saved by about 46% compared with that before the renovation, thus solving the problem of large water consumption on-site. (2) The distance between nozzles before modification is too small, resulting in serious cross interference of water jets between adjacent nozzles, and the utilization rate of nozzle water jet washing capacity is greatly reduced as shown in Figure 20. The modified nozzle water jet not only covers the surface of

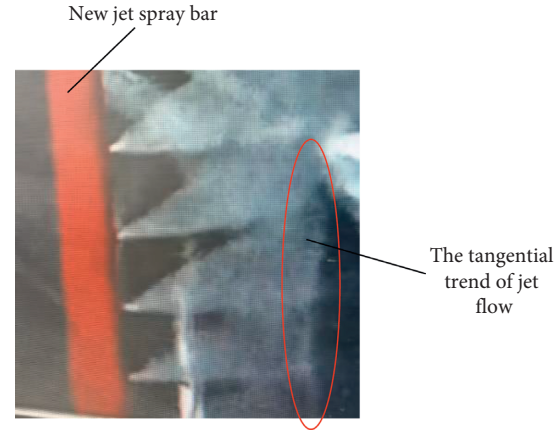

Figure 21: Nozzle jet after modification.

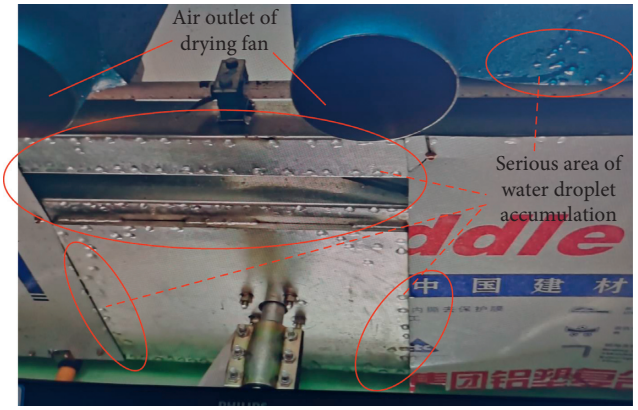

Figure 22: Water accumulation diagram caused by excessive pressure.

the automobile but also greatly improves the efficiency of each nozzle water jet. (3) When the normal angle between the nozzle jet and the automobile surface is 0° before the renovation, stains will be scattered and washed away on the automobile surface, and some stains will be washed to the washed automobile parts, causing secondary pollution to them. After reforming the normal included angle between the nozzle jet and the automobile surface to 30°, the nozzle water jet is decomposed into normal striking force and tangential pushing force as shown in Figure 21. Among them, the tangential pushing force can push the stain to the other direction of the cleaned automobile, thus preventing the secondary pollution of the automobile. At the same time, the water flow reaction force perpendicular to the automobile is effectively controlled. (4) The nozzle inlet pressure should not be too high. Too much pressure will cause the impact force of the water jet from the nozzle to offset the reaction force of the water jet rebounded from the automobile seriously, which is not conducive to the washing of stains. Moreover, some of the water jet with too much rebound force will easily splash to the roof of the workshop. Over time, water will form on the roof and continuously drip water to the top of the automobile, which is not conducive to the drying process of the automobile as shown in Figure 22.

5. Conclusion

The fan-type nozzle is more and more widely used in automobile washing industry. In order to achieve the best washing effect, this paper uses Fluent software to simulate the outflow field of the fan-type nozzle of the automobile washer, analyzes and discusses the influence of the inlet pressure of the nozzle on the spray rod, the target distance, the normal included angle between the nozzle and the body surface, and the nozzle arrangement spacing on the washing effect, and draws the following conclusions:

(1) Under the same inlet pressure, the dynamic pressure on the target surface decreases with the increase of the target distance, but too close, the target distance will cause a reverse impact force of the water jet reaching the target surface to partially offset the forward water jet reaching the target surface, making the dynamic pressure on the target surface uneven. The distance between the target surfaces should be determined by comprehensively considering the uniformity of the dynamic pressure on the target surface and keeping the target surface with large dynamic pressure. Although the larger the target distance, the weaker the washing ability of the water jet, the larger the coverage area of the water jet, the larger the area of the automobile that can be cleaned.

(2) With the increase of inlet pressure, the dynamic pressure on the target surface and the axial velocity will increase, but the growth rate will gradually decrease when reaching a certain pressure. Under the condition of a certain target distance, the area covered by water jets with different inlet pressures is basically the same.

(3) After the nozzle and the normal line of the automobile surface are inclined at a certain angle, the target surface is affected not only by normal striking force but also by tangential force, which makes stains easier to remove. Through simulation analysis, it is found that the optimal angle is to tilt the nozzle and the normal line of the automobile 30°.

(4) The target distance and nozzle distance must be matched; otherwise, it will lead to two extreme situations: one is that the automobile surface is not covered by water jet; the other case is that the water jets of adjacent nozzles interfere seriously with each other and the washing efficiency is reduced. Through numerical simulation, the matching curves among jet angle, nozzle spacing, and the distance between nozzle and automobile surface (target distance) are obtained, which provides a basic theoretical basis for the optimal design of automatic automobile washing.

(5) Through industrial tests, the correctness of the above research conclusions is verified.

Data Availability

The data used to support the findings of this study are available from the corresponding author upon request.

Conflicts of Interest

The authors declare that they have no conflicts of interest.

Acknowledgments

The work described in this paper was supported by the Foundations of Key R&D Projects of Shanxi Province (International Scientific and Technological Cooperation), China (Grant no. 201803D421041); Major Science and Technology Projects of Shanxi Province, China (Grant no. 20181101017); and Applied Basic Research Project of Shanxi Province, China (Grant no. 201701D121017).

References

[1] K. Jiang, F. Yan, and H. Zhang, "Data-driven modeling and UFIR-based outlet NO_x estimation for diesel-engine SCR systems," *IEEE Transactions on Industrial Electronics*, vol. 67, no. 6, pp. 5012–5021, 2020.

[2] K. Jiang, F. Yan, and H. Zhang, "Hydrothermal aging factor estimation for two-cell diesel-engine SCR systems via a dual time-scale unscented Kalman filter," *IEEE Transactions on Industrial Electronics*, vol. 67, no. 1, pp. 442–450, 2020.

[3] M. Kierzkowski and H. Law, "Car wash noise and EPA regulation—a case study," in *Proceedings of the ACOUSTICS 2017 Perth: Sound, Science and Society—2017 Annual Conference of the Australian Acoustical Society, AAS 2017*, Perth, Australia, November 2017.

[4] A. Nair and S. Kumanan, "Optimization of size and form characteristics using multi-objective grey analysis in abrasive water jet drilling of Inconel 617," *Journal of the Brazilian Society of Mechanical Sciences and Engineering*, vol. 40, no. 3, pp. 1–15, 2018.

[5] S. Thomas, M. Antony, and T. Dimitra, "Hard rock cutting with high pressure jets in various ambient pressure regimes," *International Journal of Rock Mechanics and Mining Sciences*, vol. 108, no. 8, pp. 179–188, 2018.

[6] D. Hu, X.-H. Li, C.-L. Tang, and Y. Kang, "Analytical and experimental investigations of the pulsed air-water jet," *Journal of Fluids and Structures*, vol. 54, pp. 88–102, 2015.

[7] S. Hannes, K. Hannes, M. Marc, and J. P. Majschak, "Investigations to increase washing efficiency with pulsed liquid jet," *Chemie Ingenieur Technik*, vol. 86, no. 5, pp. 707–713, 2014.

[8] L. M. Hlaváč, "Application of water jet description on the descaling process," *International Journal of Advanced Manufacturing Technology*, vol. 80, no. 5–8, pp. 721–735, 2015.

[9] F. Enrico, K. Sebastian, and S. Enrico, "Effect of industrial scale stand-off distance on water jet break-up, washing and forces imposed on soil layers," *Food and Bioproducts Processing*, vol. 113, no. S1, pp. 129–141, 2019.

[10] E. Helal, F. S. Abdelhaleem, and W. A. Elshenawy, "Numerical assessment of the performance of bed water jets in submerged hydraulic jumps," *Journal of Irrigation and Drainage Engineering*, vol. 146, no. 7, 2020.

[11] A. Janardanan, P. C. Ajil, P. Anju, T. V. Eldiya, and D. Davis, "Android application for car wash services," in *Proceedings of 1st International Conference on Emerging Trends and Innovations in Engineering and Technological Research*, Cochin, India, July 2018.

[12] D. Phipps, R. Alkhaddar, and M. Stiller, "Water saving in domestic car washing," in *Proceedings of World Environmental and Water Resources Congress 2013: Showcasing the Future*, Cincinnati, OH, USA, May 2013.

[13] T. T. Yu, J. Q. Wang, L. T. Wu, and Y. Xu, "Three-stage network for age estimation," *CAAI Transactions on Intelligence Technology*, vol. 4, no. 2, pp. 122–126, 2019.

[14] R. Jiang, H. Zhou, H. Wang, and S. S. Ge, "Maximum entropy searching," *CAAI Transactions on Intelligence Technology*, vol. 4, no. 1, pp. 1–8, 2019.

[15] C. L. Tang, D. Hu, and F. H. Zhang, "Study on the frequency characteristic of self-excited oscillation pulsed water jet," *Advanced Materials Research*, vol. 317–319, pp. 1456–1461, 2011.

[16] E. Fuchs, H. Köhler, and J. P. Majschak, "Measurement of the impact force and pressure of water jets under the influence of jet break-up," *Chemie Ingenieur Technik*, vol. 91, no. 4, pp. 455–466, 2019.

[17] J. W. Wen, Z. W. Qi, and S. S. Behbahani, "Research on the structures and hydraulic performances of the typical direct jet nozzles for water jet technology," *Journal of the Brazilian Society of Mechanical Sciences and Engineering*, vol. 41, no. 12, p. 570, 2019.

[18] P. A. Dumbhare, S. Dubey, Y. V. Deshpande, A. B. Andhare, and P. S. Barve, "Modelling and multi-objective optimization of surface roughness and kerf taper angle in abrasive water jet machining of steel," *Journal of the Brazilian Society of Mechanical Sciences and Engineering*, vol. 40, no. 5, pp. 1–13, 2018.

[19] J. W. Wen, C. Chen, and U. Campos, "Experimental research on the performances of water jet devices and proposing the parameters of borehole hydraulic mining for oil shale," *PLoS One*, vol. 13, no. 6, Article ID e0199027, 2018.

[20] M. Nadeem, N. Q. Tri, C. Diallo, and U. Venkatadri, "Contribution to spraying nozzle study: a comparative investigation of imaging and simulation approaches," *Pakistan Journal of Agricultural Sciences*, vol. 56, no. 1, pp. 215–224, 2019.

[21] M. Nadeem, Y. K. Chang, U. Venkatadri, C. Diallo, P. Haward, and T. Nguyen-Quang, "Water quantification form sprayer nozzle by using particle image velocimetry (PIV) versus imaging processing techniques," *Pakistan Journal of Agricultural Sciences*, vol. 55, no. 1, pp. 203–210, 2018.

[22] E. Fuchs, M. Helbig, M. Pfister, and J.-P. Majschak, "Erhöhung der Reinigungseffizienz bei der Cleaning-in-place-Reinigung durch diskontinuierliche Flüssigkeitsstrahlen," *Chemie Ingenieur Technik*, vol. 89, no. 8, pp. 1072–1082, 2017.

[23] M. W. L. Chee, T. V. Ahuja, R. K. Bhagat et al., "Impinging jet cleaning of tank walls: effect of jet length, wall curvature and related phenomena," *Food and Bioproducts Processing*, vol. 113, no. S1, pp. 142–153, 2019.

[24] B. S. Nie, H. Wang, L. Li, and J. Zhang, "Numerical investigation of the flow field inside and outside high-pressure abrasive waterjet nozzle," in *Proceedings of 1st International Symposium on Mine Safety Science and Engineering, ISMSSE 2011*, Beijing, China, October 2011.

[25] A. Kermanpur, A. Ebnonnasir, and M. Hedayati, "A novel analytical-artificial neural network model to improve efficiency of high pressure descaling nozzles in hot strip rolling of steels," *Materials Science and Technology*, vol. 23, no. 8, pp. 951–957, 2007.

[26] A. Kermanpur, A. Ebnonnasir, A. R. K. Yeganeh, and J. Izadi, "Artificial neural network modeling of high pressure descaling operation in hot strip rolling of steels," *ISIJ International*, vol. 48, no. 7, pp. 963–970, 2008.

[27] Y. T. Dou, M. Zhou, and X. J. Cai, "Nozzle arrangement of self-propelled pipeline washing nozzle," *Oil and Gas Storage and Transportation*, vol. 38, no. 6, pp. 662–666, 2019.

[28] C. T. Liu, G. Liu, and Z. X. Yan, "Study on cleaning effect of different water flows on the pulsed cavitating jet nozzle," *Shock and Vibration*, vol. 2019, Article ID 1496594, 15 pages, 2019.

[29] B. J. Liang and D. R. Gao, "Optimization of structural parameters of fan-shaped high-pressure nozzle," *Journal of Drainage and Irrigation Machinery Engineering*, vol. 38, no. 1, pp. 69–75, 2020.

[30] Y. Liu, Q. B. Ba, L. P. He, K. Shen, and W. Xiong, "Study on the rock-breaking effect of water jets generated by self-rotatory multinozzle drilling bit," *Energy Science and Engineering*, vol. 8, no. 7, pp. 2457–2470, 2020.

[31] Y.-Y. Zhang, *Fluid Mechanics*, Higher Education Press, Beijing, China, 2015.

[32] H. Kun and L. Zhenbei, *Detailed Explanation of ANSYS ICEM CFD Engineering Example*, Posts and Telecom Press, Beijing, China, 2014.
[33] J. Bingbing, Z. Xiaoxia, and G. Yan, *ANSYS ICEM CFD Basic Course and Example Explanation*, China Machine Press, Beijing, China, 2015.
[34] K. Jin, "Design and experiment research of ultrahigh pressure water jet boom washing device," Master's thesis, Dalian Maritime University, Dalian, China, 2018, in Chinese.